Carbonates Evaporites (2013) 28:281–295
DOI 10.1007/s13146-012-0114-5

REVIEW

Isotopic and hydrochemical investigation of the Grombalia deep aquifer system, northeastern Tunisia

S. Charfi · R. Trabelsi · K. Zouari · N. Chkir · H. Charfi · M. Rekaia

Accepted: 11 September 2012 / Published online: 8 November 2012

Abstract Hydrochemical and environmental isotope tracers have been used to identify the geochemical processes that affect groundwater masses in the aquifer system of Grombalia (northeastern Tunisia). The study area presents a multilayer aquifer system logged in the Quaternary and Miocene sandstones. Multi-tracer results show that the dissolution of evaporite minerals as well as the evaporation and the irrigation return flow are the main processes controlling groundwater quality. The isotopic data proves the origin of different groundwater masses as well as the natural and anthropogenic processes that control their mineralization.

Keywords Return flow · Dedolomitization · Dissolution · Cation exchange · Grombalia · Tunisia

S. Charfi (✉) · R. Trabelsi · K. Zouari
National Engineering School of Sfax,
BP 1173-3038 Sfax, Tunisia
e-mail: charfisihem1@yahoo.fr

S. Charfi · R. Trabelsi · K. Zouari · N. Chkir
Laboratory of Radio Analyses and Environment, Sfax, Tunisia

N. Chkir
Department of Geography, Faculty of Letters and Humanities,
BP 1168-3038 Sfax, Tunisia

H. Charfi
Department of English, Faculty of Letters and Humanities,
Gabes, Tunisia

M. Rekaia
Regional Commissary for Agricultural Development of Nabeul,
Nabeul, Tunisia

Introduction

In North Africa, climate aridity coupled with the increasing exploitation of groundwater resources have led to growing deficits of water resources and to a progressive degradation of groundwater quality (Bouchaou et al. 2008; Yangui et al. 2010).

In such areas, groundwater resources are often threatened by the anthropogenic contamination induced by overexploitation, which in its turn causes salinization (Ben Hamouda et al. 2010) and water-quality degradation. Moreover, irrigation based on groundwater causes the recycling of salts and their accumulation in the aquifer. One of its most pronounced impacts is the increase in the nitrate concentration derived from agriculture return flows (Hern and Feltz 1998; Hao and Change 2002). Isotopic tracers are ideal natural tracers used for solving various problems in water cycle and diverse hydrological processes, in particular in the arid and semi-arid regions (Fontes 1980; Clark and Fritz 1997; Etcheverry 2002).

The present work focuses on the Grombalia aquifer, which constitutes the main water resource in northeast Tunisia in Cap Bon Peninsula (Fig. 1). During the last few decades, the exploitation of groundwater resources has exceeded reasonable limits and reached 9.46 Mm^3 in 2000 (DGRE 2000). The number of wells and boreholes is increasing continuously to meet the increasing needs of agriculture, industry and tourism. Indeed, the Grombalia Plain is subject to erratic weather patterns characterized by successive long dry periods and short humid episodes. This long-term withdrawal has engendered several deleterious problems such as water-level decline, salinization and pollution of groundwater resources. Within this framework, the present investigation, which uses a set of geochemical and isotopic tracers, aims to provide relevant information

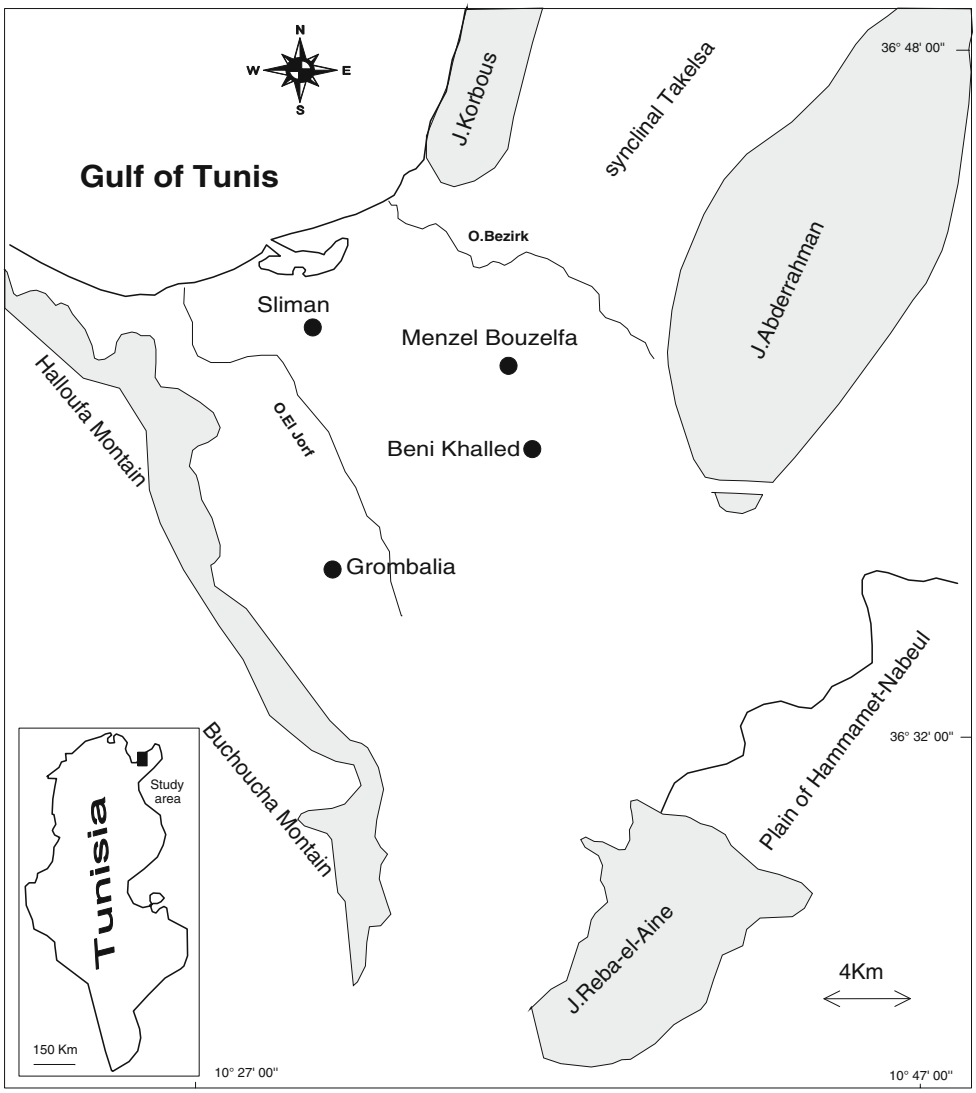

Fig. 1 Location map of the study area

concerning the origin of different groundwater masses as well as the natural and anthropogenic processes that control their mineralization, which will contribute to the sustainable management of groundwater resources in the study area.

Study area

The study area is located between the longitudes 10° 27′00″ and 10° 47′00″ and the latitudes 36° 29′00″ and 36° 42′00″. It is limited in the north by the Gulf of Tunis, to the northeast by Takelsa syncline, to the east by Abderrahman Mountain and the oriental coastal highlands, and to the south by the Plain of Hammamet (Fig. 1).

The Grombalia Plain is characterized by a semi-arid to sub-humid Mediterranean climate. This type of climate is the result of the convergence of several climatic parameters: rainfall is variable, in time and space, with an annual average value of 500 mm. The mean annual temperature is around 18.7 °C. The potential evapotranspiration is higher in summer as a result of the increase in temperature and the decrease in the air moisture.

Geological and hydrogeological setting

A previous geological survey (Castany 1948) shows that the old Quaternary terraces outcrop on the south of the Plain of Grombalia, while, recent terraces are located on the northern part. The formations' lithology becomes more and more marine marking the transition from the continental deposits (sands, sandstones, pebbles and gravel) to coastal deposits toward the Gulf of Tunis. In conclusion, the study area corresponds to a rift that had begun to open since the Oligocene and whose border faults affecting Miocene and Pliocene deposits would probably have stopped moving in the late Post-Pliocene period (Ben Salem 1992). From a tectonic point of view, there are two

major normal faults oriented NNW–SSE and NNE–SSW, which have contributed to the collapse of the Grombalia Plain and given rise to a rift. These two faults constitute the natural boundaries of the study area (Ben Ayed 1986) (Fig. 2).

The Plain of Grombalia is formed by subsidence of more than 500 m of Quaternary deposits. From the lithological point of view, the Quaternary is composed of alternating layers of permeable sand and relatively impervious marl layers forming a multilayered aquifer system. The different deep aquifer levels communicate with each other more or less freely, and also with the shallow aquifer levels. The hydraulic communication between these different levels is due to the discontinuity of marl layers (Ennabli 1980) (Fig. 3).

The piezometric map of the aquifer of Grombalia was established using measurements of hydraulic head during the sampling campaign conducted during the month of February 2005 (Mahmoudi 2005). The map shows that Grombalia groundwater flows through two main directions: (1) from the northeast to the southwest and (2) from the southeast to the northwest on the Mediterranean Sea (Fig. 4). The highest values of 70–60 m were measured in northeastern and southeastern parts of the plain and the lower levels from 25 m were located downstream the basin near Grombalia Town. The recharge of the deep aquifer is ensured mainly by direct infiltration of rainwater through permeable layers at two regions:

- The first one is located to the northeast of the plain, corresponding to the eastern foothills of the Abderrahman relief.
- The second one is situated in the southeastern part of the Hammamet Plain

Groundwater sampling and analyses

The qualitative and quantitative characterization of the deep groundwater of Grombalia has involved field investigations and laboratory analyses. Thus, 55 water samples were collected during March 2005 from deep wells whose depth varied from 60 to 150 m, chosen according to their geographic locations and lithology formations in such a way that they represent different hydrochemical types and distinct hydrogeological conditions of the Grombalia aquifer (Fig. 5). All samples for major chemical analyses were collected in low density polyethylene bottles and filtered in the laboratory through 0.45 μm membrane filters.

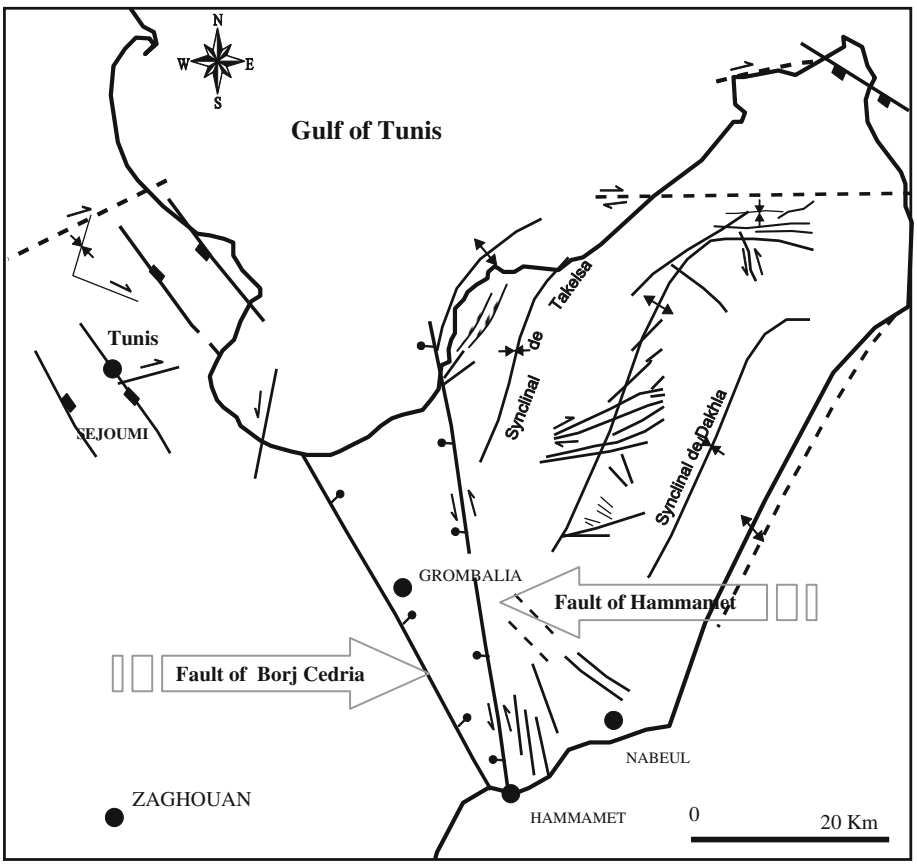

Fig. 2 Structural map of the Peninsula of Cap Bon (Touati et al. 1994)

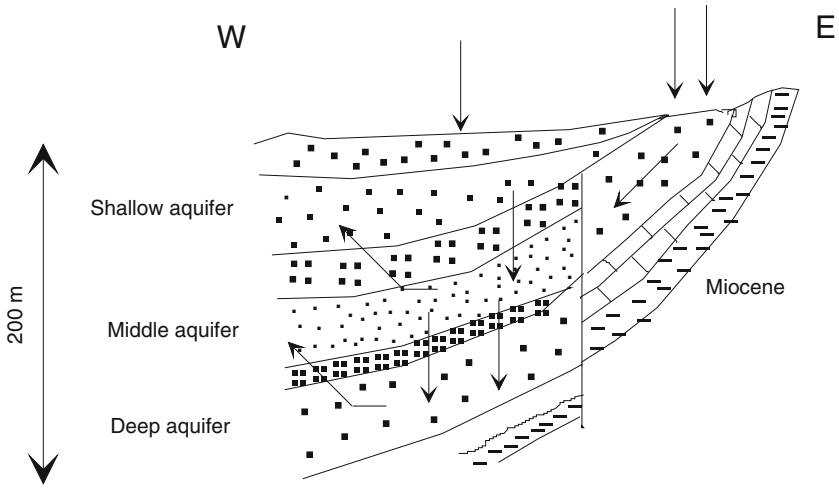

Fig. 3 Hydrogeological cross of the Grombalia aquifer (Ennabli 1980)

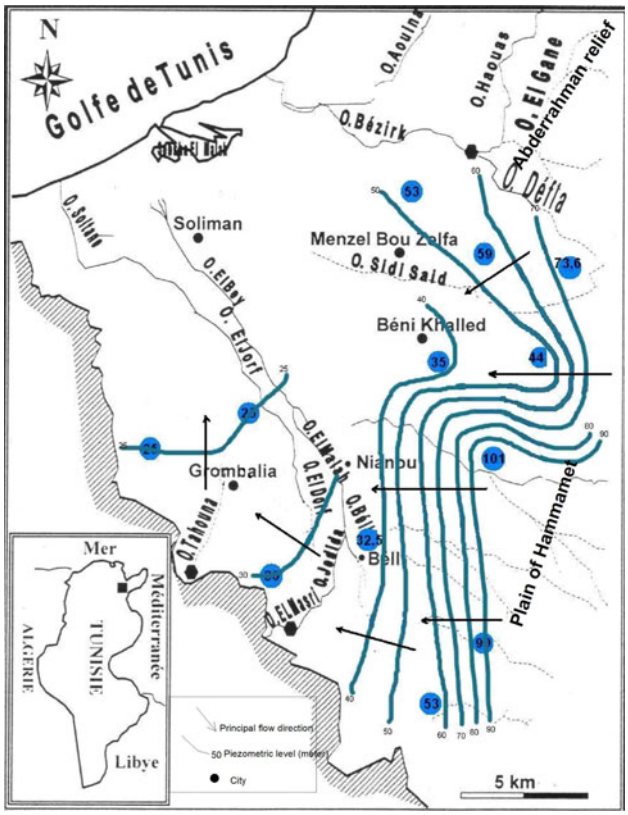

Fig. 4 Piezometric map of the deep aquifer (2005) (Mahmoudi 2005)

Temperature, pH and electrical conductivity (EC) of sampled groundwater were measured in the field. Chemical analyses of water samples were carried out in the Laboratory of Radio-Analysis and Environment of the National School of Engineers of Sfax, Tunisia. Calcium, Mg, Na, K, Cl, SO_4 and NO_3 were analyzed by liquid-ion chromatography (HPLC) on a Waters chromatograph equipped with columns IC-PakTM CM/D for cations, using EDTA and nitric acid as eluent, and on a Metrohm chromatograph equipped with columns CI SUPER-SEP for anions using phthalic acid and acetonitric as eluent. The overall detection limit for ions was 0.04 mg/l. The total alkalinity (as HCO_3) was determined by titration with 0.1 N HCl solution using methyl orange indicator.

Stable isotope ($\delta^{18}O$, $\delta^{2}H$) analyses were performed in the laboratory of the International Agency of Atomic Energy (IAEA) in Vienna, using standard CO_2 equilibration (Epstein and Meyada 1953) and the zinc reduction techniques (Coleman et al. 1982), respectively, followed by analysis on a mass spectrometer. Oxygen and hydrogen isotope analyses were reported to δ notation relative to Vienna Standard Mean Oceanic Water (VSMOW), where $\delta = [(Rs/RVSMOW) - 1] \times 1{,}000$, Rs represents either the $^{18}O/^{16}O$ or the $^{2}H/^{1}H$ ratio of the sample, and RSMOW is $^{18}O/^{16}O$ or the $^{2}H/^{1}H$ ratio of the SMOW. Typical precisions are ± 0.1 and ± 1 ‰ for oxygen-18 and deuterium, respectively. The $\delta^{13}C$ contents of total dissolved inorganic carbon (TDIC) was measured using isotope ratio mass spectrometry and reported in ‰ versus PDB (Coplen 1996) with a typical analytical uncertainty of ± 0.1 ‰. All carbonate species were converted to CO_2 by acidifying the water sample.

Carbon-14 concentrations were also measured in the Sfax School of Engineers through benzene synthesis and liquid scintillation spectrometry (Fontes 1971). Results are expressed as percent modern carbon (pmc). The analytical uncertainty is between 1 and 1.5 pmc for ^{14}C.

Groundwater chemistry

In situ measurements and TDS interpretation

Chemical and isotope analyses of the investigated groundwater samples are represented in Table 1.

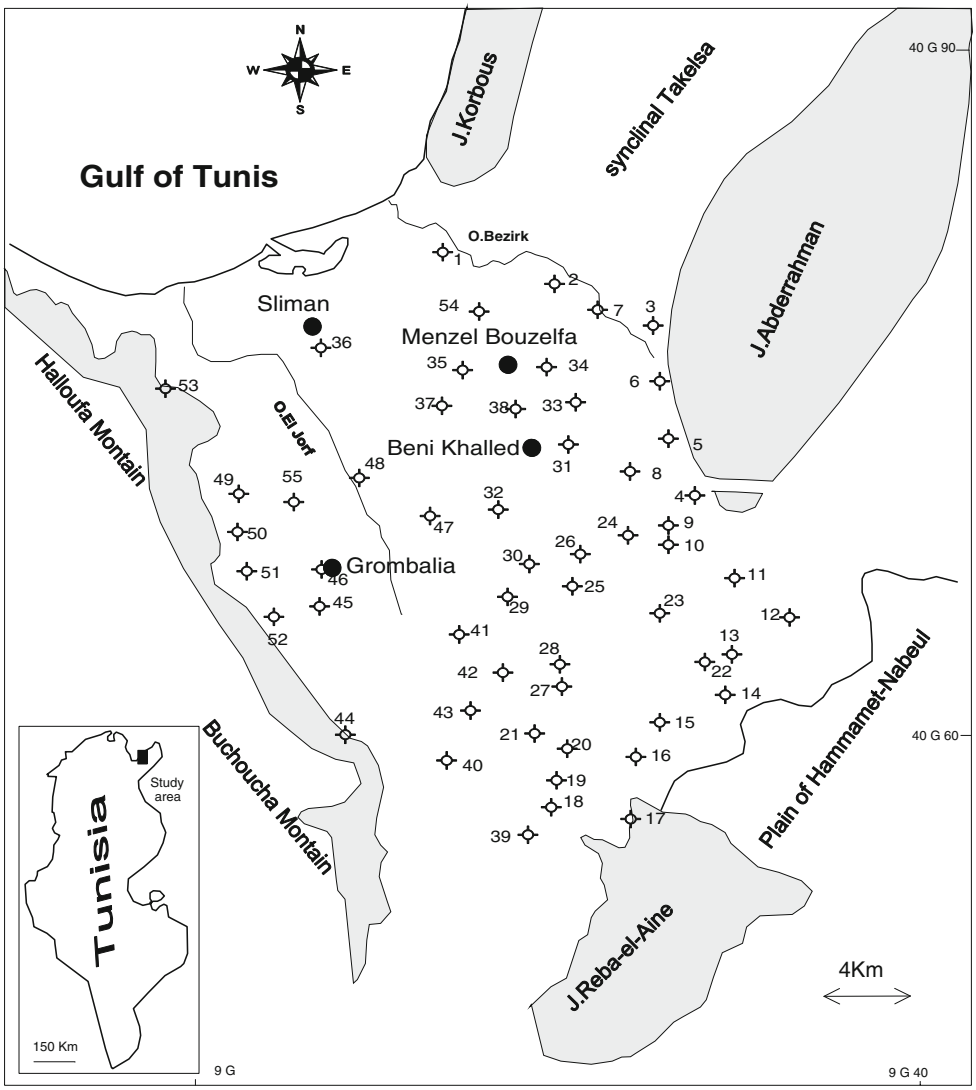

Fig. 5 Sampling map

The groundwater pH values range from 6.09 to 8.19 and the temperature varies within a wide range of 14–26.7 °C, indicating the combination of several factors such as residence time, recharge rate and groundwater depth. The electrical conductivity ranges from 0.59 to 3.86 mS/cm.

The spatial distribution of the groundwater salinity shows a clear increase according to groundwater flow direction. The lowest salinity was observed in the southeastern and northeastern bands of the basin corresponding to the recharge areas. Salinity increases progressively toward the Mediterranean Sea in the Gulf of Tunis (discharge area), as a result of the scarcity of recharge in these regions and the relatively long-term water–rock interaction. Nevertheless, unexpectedly high salinities were measured in some deep wells located in the eastern and southern parts of the basin. These high salinities are not in agreement with the general groundwater flow. This situation could be explained by the impact of evaporitic deposits and the use of nitrogen fertilizers.

Water types

The chemical compositions of Grombalia groundwater samples are presented in Piper diagram (Fig. 6). It allows one to recognize the following hydrochemical types, based on the prevailing anion and cation:

(1) Na(K)–Cl, comprising samples 1, 7, 8, 10, 11, 12, 16, 19, 21, 25, 26, 27, 29, 30, 31, 35, 36,37, 40, 44, 46, 48, 49, 51, 52, 53 and 54, whose total ionic salinity (TIS) varies from 23 to 146 meq/L. It is the most represented chemical type of water and likely originated from halite dissolution and possibly seawater ingression in coastal areas.

Table 1 Isotopic and geochemical data for Grombalia deep aquifer

No.	Cl	NO_3	SO_4	CO_3	HCO_3	Na	K	Mg	Ca	TDS	^{18}O	^{2}H	^{14}C	^{13}C	EC	*T*	pH
1	449.8	55.6	211.7	0	317.2	311.6	4.1	38.3	142.2	1,739			56.5	−13	1.94	23	7.33
2	517.8	81	110.0	0	329.4	162.0	4.8	39.6	242.0	1,663	−5.2	−28.4	96.6	−13.1	2.15	22.5	7.01
3	135.5	67.1	5.3	0	305.0	70.0	3.1	18.1	115.5	640			89.7	−14.3	1.009	20.7	6.93
4	692.6	91.5	330.4	0	122.0	270.0	3.2	52.7	321.2	1,999	−4.4	−32			2.08	23	7.13
5	400.2	114	137.6	0	372.1	165.0	2.1	29.2	220.6	1,609	−5.6	−31.3	100	−14.4	1.679	21.9	7.07
6	225.7	13.2	68.4	0	353.8	93.0	1.9	19.3	136.0	759			82.5	−14.3	1.31	20.6	6.94
7	299.9	0	158.7	12	311.0	210.2	12.2	47.1	60.7	1,000	−5.5	−31.4			1.831	23.3	7.86
8	268.1	0	65.8	0	366.0	154.5	23.0	31.0	122.4	880	−5.8	−32.9		−13.5	1.416	23.6	7.42
9	591	50.2	156	0	341.6	218	3.3	68.2	198.4	2,129	−4.7	−32.5	75.6	−11.6	2.89	19.7	7.2
10	345.7	0	74.2	36	329.4	174.4	2.5	65.0	95.8	1,070	−5.6	−31.8	50	−12.3	1.932	21.8	7.46
11	385.7	0	449.1	0	402.6	397.8	20.2	58.9	75.6	1,784	−5.2	−30.9	52.7	−13	2.34	21.2	7.48
12	174.1	75.8	27.4	0	274.5	135.1	27.2	17.9	77.2	1,102			43.5	−12.3	1.211	22	7.4
13	349.8	10.4	41.2	0	280.6	93.4	1.4	21.0	174.4	1,060	−5.8	−32.5	98.2	−14.4	1.509	21.4	7.04
14	415.8	66.5	123.3	0	420.9	179.5	6.8	19.2	241.4	1,841			97.6	−14	2.07	21	6.09
15	130.6	27.3	12.1	18	311.1	69.2	2.0	31.8	89.6	670			74	−12.6	1.119	21.4	7.13
16	300.6	47	88.3	0	512.4	145.8	9.5	58.2	130.8	1,204	−4.5	−33.2	94.7	−12	2.1	17.2	7.76
17	369.0	0	511.3	0	231.8	102.1	3.7	101.3	215.5	1,480	−5.4	−30.4	67	−11.1	2.02	22.2	7.34
18	55.0	7.12	69.1	12	262.3	51.9	5.0	34.7	44.1	460	−5.5	−31.9	81	−12.2	0.753	22.6	7.79
19	199.4	37.9	64.3	0	250.1	103.0	10.0	31.5	80.9	1,109			80.3	−12.3	1.086	22.7	7.6
20	42.6	10.7	41.4	30	157.9	30.6	4.7	18.3	54.8	375	−5.7	−31.5	70.5	−11.9	0.595	21.3	7.93
21	217.2	49.8	167.6	0	231.8	133.2	3.2	38.8	108.2	930	−5.3	−30.5	93	−11.4	1.333	25.5	7.76
22	224.1	42.2	73.6	0	366	91.6	2.3	30.5	165.9	1,025	−5.1	−33.8			1.521	20.2	7.75
23	224.5	16.4	47.9	0	335.5	98.4	3.4	43.1	93.5	780	−5.7	−31.6	63	−13.1	1.285	22.9	7.38
24	632.4	0	174.7	0	311.1	234.5	0.0	46.1	223.1	1,530	−5.6	−31.5	69.5	−12.7	2.54	22.5	7.3
25	426.6	0	247.2	30	237.9	288.2	10.9	50.1	85.1	1,340	−5.9	−34.7	52	−13.1	2.33	21.9	7.45
26	238.0	0	209.3	24	347.7	186.2	11.6	62.3	61.9	1,130	−5.9	−33.7	19.7	−11.5	1.93	26.7	7.35
27	956.0	0	783.5	0	664.9	490.0	13.2	239.5	298.8	3,163			80	−13.5	3.86	22	7.09
28	181.3	22.2	33.5	30	323.3	104.9	5.6	42.1	62.9	730			26	−12.5	1.164	21.8	7.6
29	502.8	0	302.0	0	341.6	212.4	4.6	87.7	148.1	1,987	−4.9	−28.7	66.5	−11.3	2.29	22	7.25
30	345.9	21	264.3	0	359.9	240.3	22.9	55.8	109.9	1,370	−5.5	−32	51	−13	2.15	22	7.31
31	484.4	51.7	224.2	0	359.9	250.4	9.2	48.1	161.0	1,643	−5.6	−31.3	46.8	−12.1	1.863	21.7	7.27
32	446.8	36.1	365.9	0	323.3	259.6	7.8	55.0	199.9	1,882	−4.3	−25.8	109.3	−12.3	1.29	21.7	7.12
33	109.1	48.9	38.1	0	298.9	70.7	1	12.9	99.8	657	−5.1	−36.2	81.4	−13.1	1.73	20.6	7.44
34	348.5	99.5	70.0	0	329.4	95.8	7.2	55.7	163.0	1,593	−5.6	−31.6	83	−13.4	1.596	19.5	7.05
35	385.9	213	300.2	0	237.9	255.6	18.6	34.7	195.8	1,582	−4.8	−25.6	84	−11.9	2.45	22.3	7.44
36	1,144	0	569.3	0	329.4	572.6	16.1	97.7	235.5	3,400	−4.3	−31.1	111.4	−12.1	4.86	19.5	7.59
37	1,546	256	809.8	0	359.9	889.4	16.6	108.9	556.0	4,659	−5.4	−30.3	46.6	−11	1.943	22.2	7.17
38	504.1	190	258.3	0	329.4	245.6	3.7	32.5	290.3	2,121	−3.5	−27.8	78	−12.5	2.13	22.4	7.54
39	79.3	23.2	67.1	0	231.8	47.2	1	22.1	68.2	487	−4.4	−34	65.7	−11.6	0.764	20.9	8.19
40	500.7	21.8	455.1	0	312.5	263.9	4.5	86.7	206.2	1,965	−4.9	−33.6	87.4	−11.5	2.83	19.2	7.51
41	85.5	14.6	88.9	0	250.3	102.2	3.1	26.8	49.2	550	−4.9	−32.6	17.5	−9.94	1.002	20.7	7.45
42	85.8	27.6	62.6	0	300	72.9	2.2	35.7	72.6	600	−4.3	−28.5	56.5	−10.2	1.011	19.6	7.97
43	89.6	27.9	45.2	12	244.0	65.2	9.8	39.6	54.0	470	−5	−30.1	60	−11.9	1.009	21.9	7.38
44	311.1	0	121.1	0	488.0	198.8	13.2	79.8	112.3	1,205			44.5	−9.67	1.97	21.2	7.81
45	659.5	0	479.1	36	128.1	255.6	8.4	116.6	233.7	2,010	−5.4	−29.5		−12.5	2.31	21.6	7.25
46	823.1	28.8	418.1	0	298.9	409.5	0.0	100.0	271.2	2,360	−5.3	−31	71	−13	3.59	22.7	7.1
47	170.9	0	116.3	0	402.6	196.5	5.1	30.5	63.5	931	−4.8	−34.1	20.8	−9.5	1.541	21.6	7.4

Table 1 continued

No.	Cl	NO_3	SO_4	CO_3	HCO_3	Na	K	Mg	Ca	TDS	^{18}O	^{2}H	^{14}C	^{13}C	EC	*T*	pH
48	681.4	0	312.9	0	384.3	401.5	19.8	83.0	127.1	1,804	−5.4	−29.7	19.7	−8.87	2.98	25	7.46
49	851.9	0	191.8	0	292.8	385.5	100.9	61.3	165.7	1,740	−5.5	−31	27.3	−10	3.04	23.5	7.31
50	598.8	53.4	260.6	0	427.0	248.2	0.0	66.9	250.4	1,815	−5.5	−31.6	78.3	−13	2.73	24.4	6.91
51	495.6	53.3	174.1	0	359.9	297.6	5.4	52.4	124.8	1,798	−5	−35.5			3.52	19.6	7.64
52	503.2	0	529.2	0	400.2	346.3	5.5	76.2	194.8	2,154	−5.1	−33.7	83.4	−11.8	3.17	19.5	7.32
53	542.7	142	139.5	0	384.3	269.4	1.6	51.7	205.5	1,854	−4.4	−30.9	77.2	−12	2.68	23.6	7.41
54	284.3	22.1	134.1	0	305	206.4	10.9	27	85.3	1,017	−4.9	−34.9	19.1	−11	1.724	14	7.68
55	143.6	0	82.9	60	317.2	96.4	8.3	48.7	72.5	630	−5.8	−33.6		−12.6	1.063	21.5	7.4

Geochemical data (mg l^{-1})

Electrical conductivity: EC (mS cm^{-1})

Temperature: T (°C)

Total dissolved salinity: TDS (mg l^{-1})

$\delta^{18}O$ and $\delta^{2}H$ values of H_2O: ‰ versus VSMOW

^{13}C of DIC: ‰ versus VPDB

^{14}C activity: percent modern carbon (pmc)

(2) Ca–Cl, including samples 2, 4, 5, 6, 9, 13, 14, 22, 23, 24, 34, 38, 45 and 50, whose TIS ranges from 26 to 63 meq/L. This type of water is typically produced by ion exchange, due to interaction of Na–Cl waters with ion exchangers whose sites are initially saturated by Ca^{2+} ion. During this process, the aqueous solution acquires Ca^{2+} ion and loses an equivalent amount of Na^{+} ion, without any change in salinity.

(3) Ca–SO_4, represented by samples 17 only, whose TIS is equal to 48 meq/L. This hydrochemical facies is generated by dissolution of Ca–sulfates, such as gypsum and anhydrite.

(4) Ca–HCO_3, comprising samples 3, 15, 20, 33, 39 and 42, whose TIS varies from 11 to 20 meq/L. The composition of this type of water, also characterized by high contents of Mg and alkalis, is chiefly governed by rock dissolution, driven by conversion of aqueous CO_2 in the HCO_3^{-} ion.

(5) Mg–HCO_3, represented by samples 18 and 43, whose TIS is equal to 17 and 15 meq/L, respectively. The chemistry of these two waters, also characterized by high contents of Ca and alkalis, is mainly controlled by rock dissolution, driven by conversion of aqueous CO_2 in the HCO_3^{-} ion.

(6) Na–KMg–HCO_3, including samples 28, 41, 47 and 55, whose TIS ranges from 18 to 28 meq/L. This hydrochemical facies may have originated by either freshening (that is by flux of Ca–HCO_3 waters in aquifers previously affected by seawater ingression; during this process, the aqueous solution acquires Na^{+} ion and loses an equivalent amount of Ca^{2+} ion, without any change in salinity) or dissolution of Na(K)-bearing silicate minerals, driven by conversion of aqueous CO_2 in the HCO_3^{-} ion.

Origin of mineralization

Groundwater mineralization of the Grombalia aquifer occurred by several processes. Indeed, the interaction between water and rocks in different formation leads to the dissolution of some chemical elements. Also, evaporation and the cation exchange process contribute to the increase in TDS.

Figure 7 represents the evolution of major element contents as a function of the TDS established to determine major elements that contribute to water mineralization. The Grombalia groundwater shows that Na, Cl, Ca, Mg and SO_4 are the main contributors to groundwater mineralization.

The saturation indices are calculated with the aid of WATEQ-F program (Plummer et al. 1976).

The binary diagram Na/Cl shows a positive correlation between these two elements ($R^2 = 0.86$); the majority of samples plot on the 1:1 (Na:Cl) line (Fig. 8). The negative saturation indices of Grombalia groundwater indicates undersaturation with respect to the halite (Fig. 9).Thus, halite dissolution could contribute to groundwater mineralization. We cannot confirm or exclude the phenomenon of seawater intrusion, because the piezometric map is incomplete due to the absence of deep piezometers near the coast.

The variation diagram of (Ca + Mg) versus (HCO_3 + SO_4) shows a correlation between these two variables ($R^2 = 0.71$) (Fig. 10). Thus, the dissolution of carbonate minerals (calcite and dolomite) and/or evaporite minerals (gypsum and anhydrite) plays an important role in

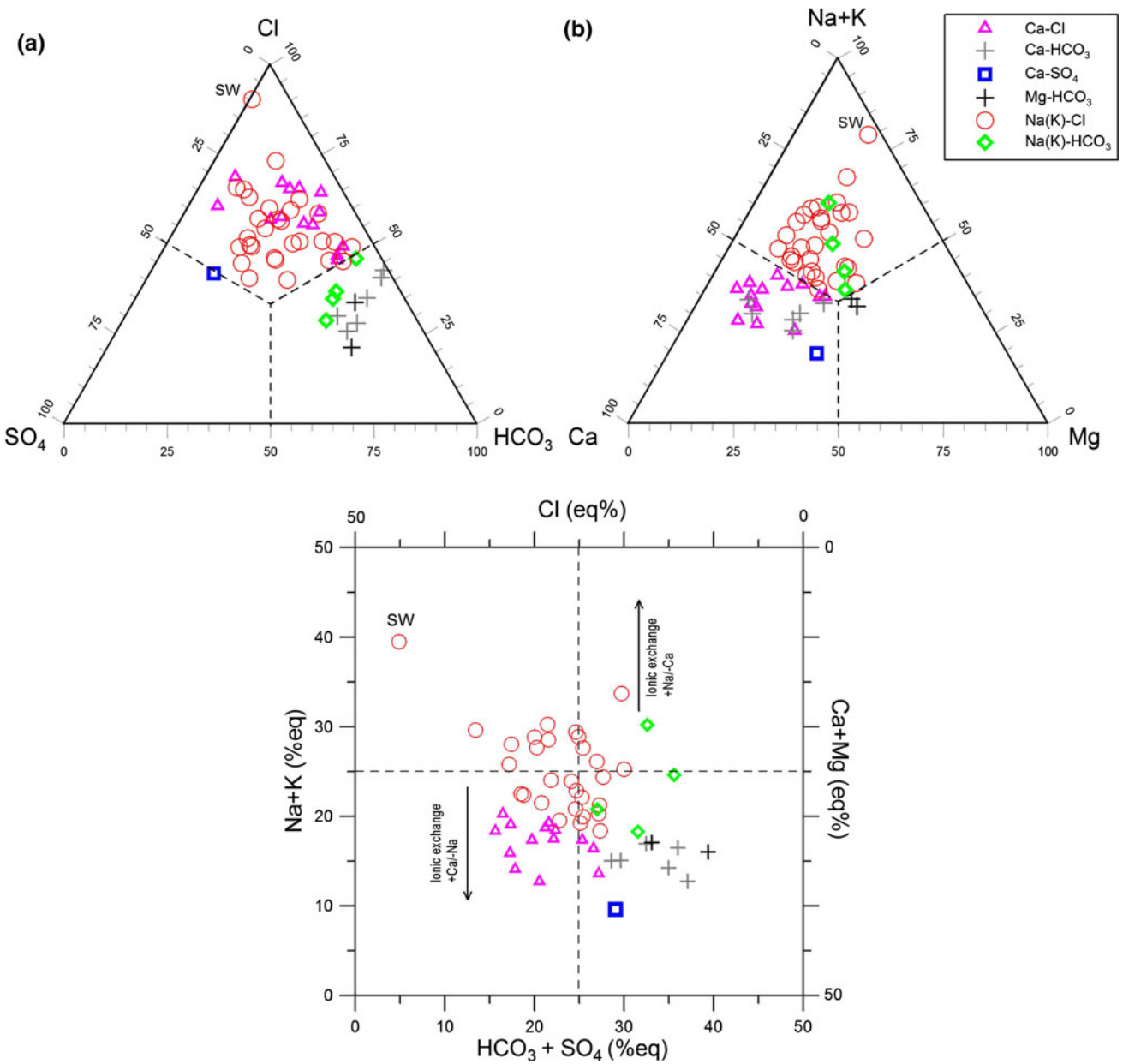

Fig. 6 Piper diagram of the deep aquifer

the acquisition of the mineralization of Grombalia groundwater.

The diagram of Ca/SO_4 (Fig. 11) shows a positive correlation between these two elements. The negative saturation indices of Grombalia groundwater indicates undersaturation with respect to the gypsum and anhydrite (Fig. 12).Thus, the dissolution of the anhydrite and gypsum minerals presents an essential role in the acquisition of the mineralization of Grombalia groundwater.

The Ca versus SO_4 plot shows that all the samples (apart one) plot along the $Ca=SO_4$ line or above it. Therefore, there is an excess of calcium. This could be due to either Na–Ca exchange or loss of sulfate due to bacterial sulfate reduction. In any case, precipitation of calcite is likely to occur; this process is triggered by either increase in Ca (in the case of cation exchange) or increase in HCO_3 (in the case of bacterial sulfate reduction).

The phenomenon of bacterial sulfate reduction cannot be confirmed or excluded due to the absence of information on redox potential (Eh).

The phenomenon exchange is confirmed through the plot of $(Na + K)–Cl$ versus $[(SO_4 + HCO_3) - (Ca + Mg)]$ that exhibits an inverse proportional evolution with a slope of about -1 (Carol et al. 2009; Abid et al. 2009) (Fig. 13).

The binary diagram between Ca and HCO_3 (Fig. 14) shows a poor correlation between these two major

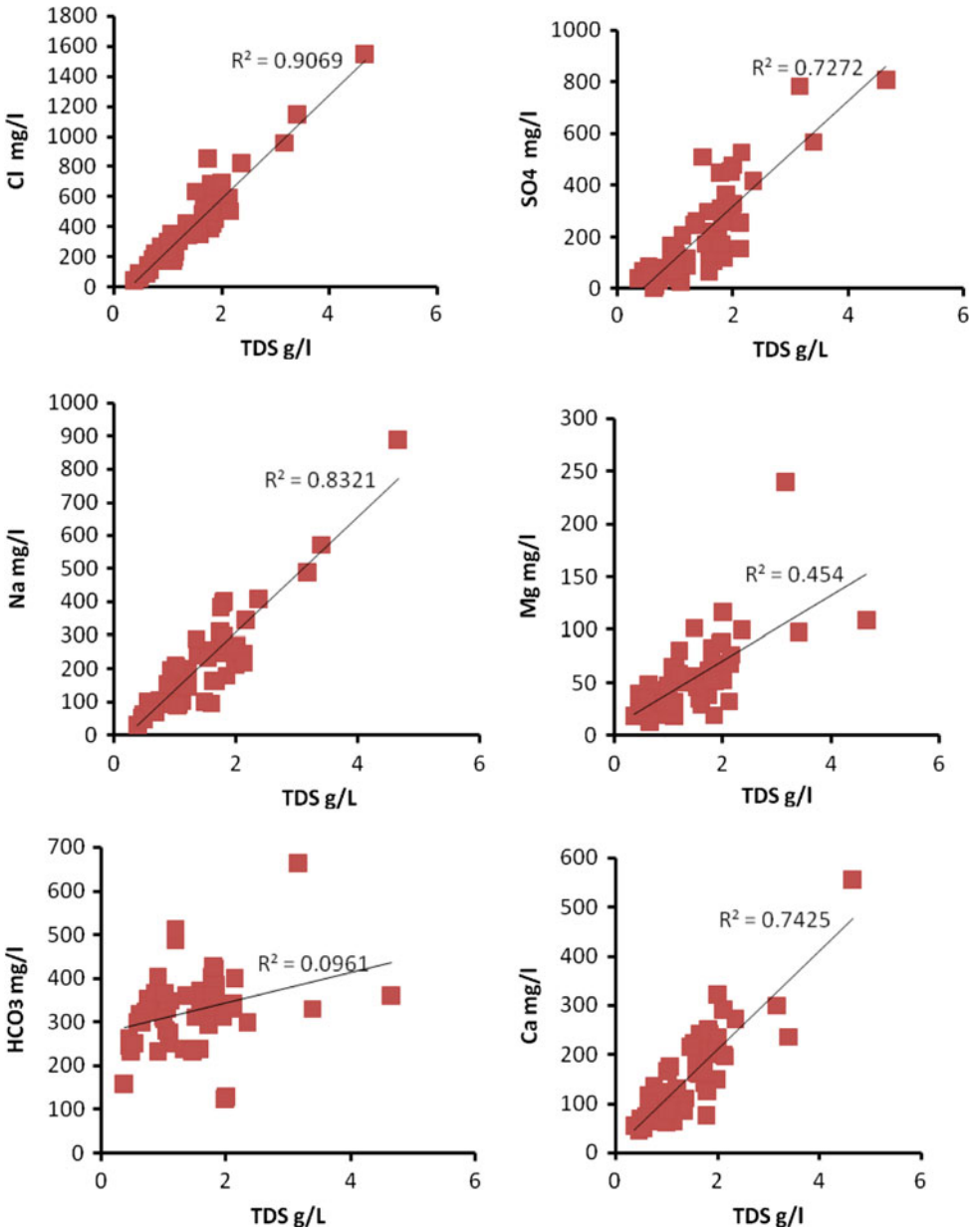

Fig. 7 Major elements versus TDS relationships

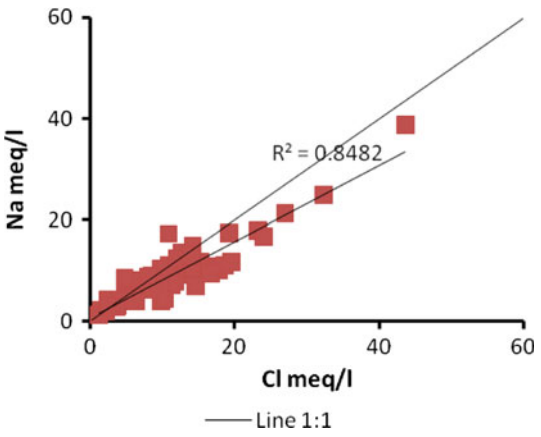

Fig. 8 Plot of Na versus Cl

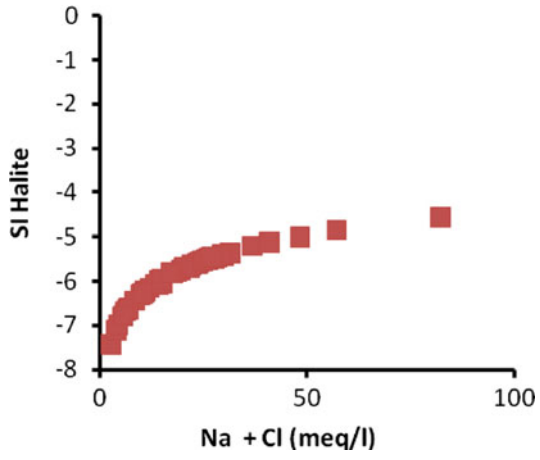

Fig. 9 Plot of (Na + Cl) versus SI of halite

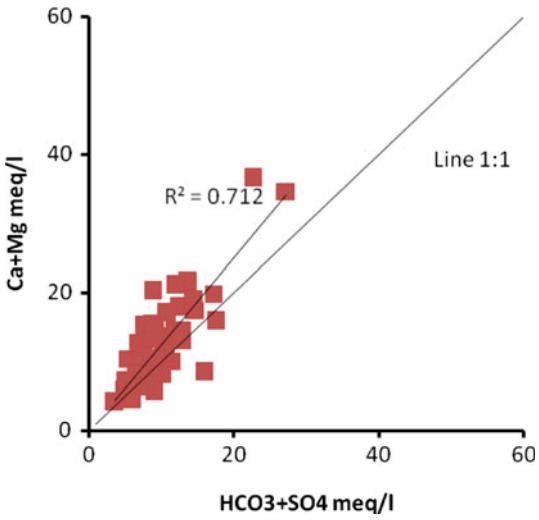

Fig. 10 Plot of (HCO_3 + SO_4) versus (Ca + Mg)

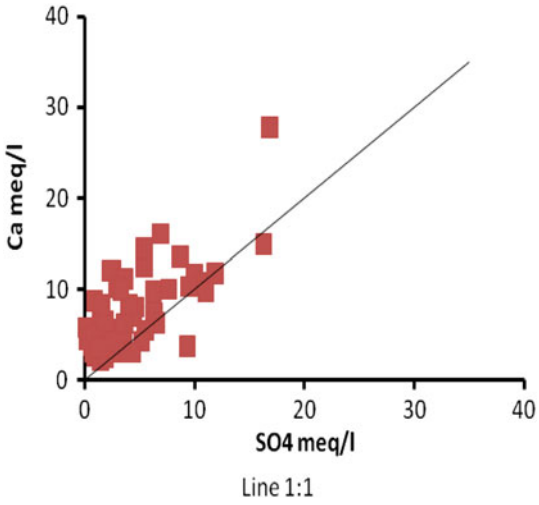

Fig. 11 Plot of SO_4 versus Ca

components. In their present state, sampled waters cannot dissolve calcite and dolomite, as they are oversaturated or close to equilibrium with respect to these minerals. Thus, Ca appears to be mainly derived from either dissolution of anhydrite and gypsum or ionic exchange or both processes.

The diagram of Mg/SO_4 (Fig. 15) shows a positive correlation between these two elements suggesting a common origin, possibly related to dissolution of epsomite ($MgSO_4 \cdot 7H_2O$). Samples located above the line of slope 1 show an excess of Mg, which might be explained by cation exchange with clay minerals or incongruent dissolution of dolomite or dedolomitization (Edmunds et al. 1982; Appelo and Postma 1993).

The relative excess of Ca could be explained by the existence of another source of Ca, perhaps in relation with

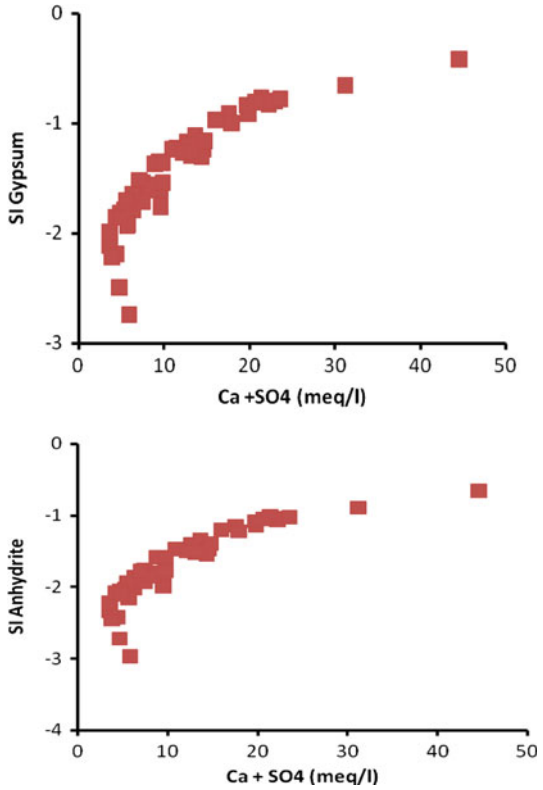

Fig. 12 Plot of (Ca + SO_4) versus SI of gypsum and (Ca + SO_4) versus SI of anhydrite

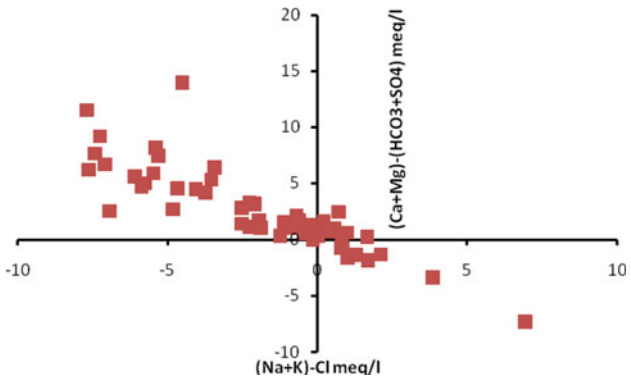

Fig. 13 Plot of (Na + K) − Cl versus (HCO_3 + SO_4) − (Ca + Mg)

Ca $(NO_3)_2$ fertilizer (Stigter et al. 2006). Therefore, the use of fertilizers could contaminate groundwater resources by return flow from irrigation water.

Nitrate content

The nitrates concentrations in the groundwater of Grombalia diverge outside a large range from 0 to 256 mg/l. It is an indicator of anthropogenic pollution in areas of high agricultural activity and reflect the return of irrigation water in the aquifer system studied.

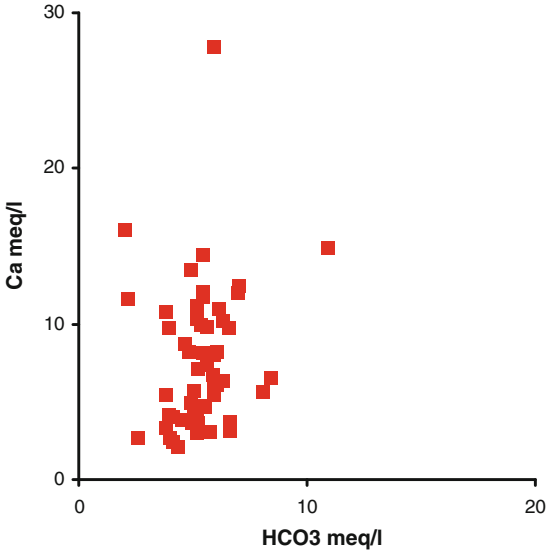

Fig. 14 Plot of Ca versus HCO_3

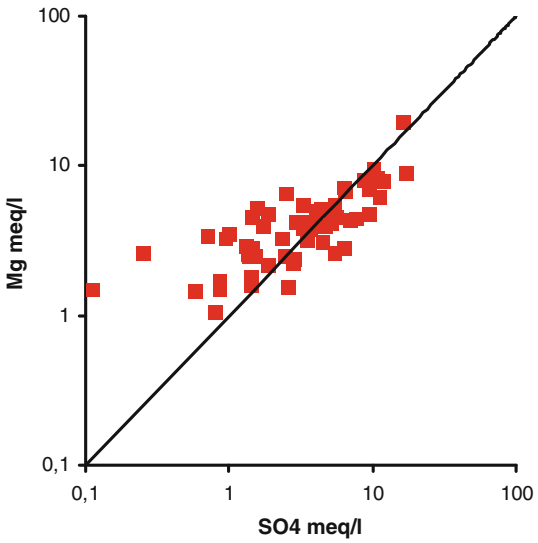

Fig. 15 Plot of Mg versus SO_4

Water samples characterized by high nitrate concentrations exceeding 50 mg/l reflect the presence of agricultural influences that introduce a long-term risk of groundwater pollution by excess fertilizers and pesticides. Indeed, there is a weak positive relationship correlation between NO_3 and Ca (Fig. 16) suggesting that dissolution of Ca $(NO_3)_2$ fertilizers might contribute most of the nitrate and some calcium to the aqueous solutions of the considered aquifer (Stigter et al. 2006). Therefore, the nitrate contamination is derived mainly from irrigation return flows.

The study area is an agricultural area characterized by a low density of septic tank; for this reason, the different sources of NO_3 at the origin of wastewater are excluded.

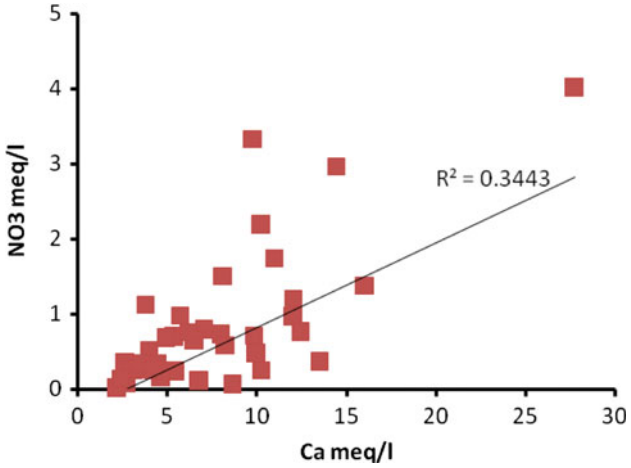

Fig. 16 Plot of NO_3 versus Ca

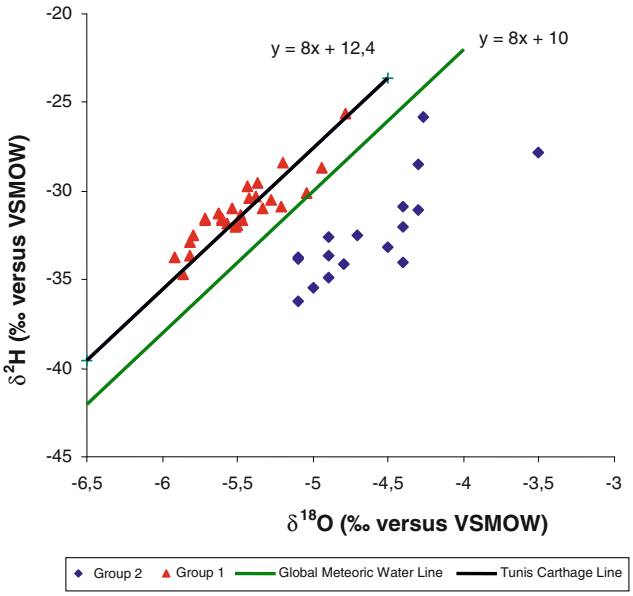

Fig. 17 $\delta^{18}O/\delta^{2}H$ diagram

Isotopic composition of groundwater

Stable isotopes of water molecule ($\delta^{18}O$ and $\delta^{2}H$)

The use of oxygen-18 and deuterium isotopes in hydrogeology offers information on the origin and movement of groundwater. It can offer an evaluation of physical processes that affect water masses, such as evaporation and mixing (Geyh 2000). The isotopic compositions of the groundwater samples from the Grombalia deep aquifer range from −6 to −3.5 ‰ for $\delta^{18}O$ and from −36.2 to −25.6 ‰.for $\delta^{2}H$. The correlation diagram of $\delta^{18}O/\delta^{2}H$ (Fig. 17) shows the position of all samples relative to the Global Meteoric Water Line (GMWL: $\delta^{2}H = 8\ \delta^{18}O + 10$) (Craig 1961) and the Local Meteoric Water

Line of the Tunis-Carthage (LMWL: $\delta^2H = 8\ \delta^{18}O + 12.4$) (Zouari et al. 1985). However, in detail, these groundwater samples can be divided into two groups.

- The first group shows that the precipitation ensuring the recharge of the Grombalia aquifer originates from a mixture of oceanic and Mediterranean vapor masses. This indicates that they are not significantly affected by evaporation, which implies rapid infiltration of rainfall waters. This rapid infiltration is consistent with the relatively high hydraulic conductivity that characterizes the natural recharge area of the Grombalia aquifer.
- The second group which is placed below (or to the right of) the GMWL comprises waters relatively enriched in oxygen-18 and relatively depleted in deuterium with respect to the GMWL. This spread of points might be ascribed to surface evaporation, indicating either slow infiltration of rainfall waters through low-permeability soils or return flow of relatively evaporated irrigation water.

The water fraction lost by evaporation may also be evaluated using the equation given by Gonfiantini (1986)

$$X = (\delta s - \delta i)(1 - h + \Delta\varepsilon)/(\delta s + 1)(\Delta\varepsilon + \varepsilon/\alpha) + h(\delta a - \delta s)$$

where X is the percentage water loss by evaporation, δs is the mean isotopic value of the aquifer water, δi is the mean isotopic value of the input aquifer water, δa is the mean isotopic value of the water vapor (−18.8 and −119.1 ‰ for $\delta^{18}O$ and δ^2H, respectively), h is the mean relative humidity, α is the equilibrium fractionation factor at 25 °C (1.0093 and 1.08 for $\delta^{18}O$ and δ^2H, respectively), and $\Delta\varepsilon$ is the kinetic enrichment factor, evaluated here as $\Delta\varepsilon\ ^{18}O\ ‰ = 14.2(1 - h)$ and $\Delta\varepsilon\ ^{2}H\ ‰ = 12.5(1 - h)$, as most frequently encountered condition in nature (Gonfiantini 1986; Kattan 2007) and $\varepsilon = \alpha - 1$.

Based on the Gonfiantini (1986) equation, the fraction of evaporated water from Grombalia aquifer ranges between 0.24 and 0.65%, using ^{18}O. These results as expected to reflect the semi-arid conditions prevailing in this area.

Note here that all estimates include also the fraction of evaporated water derived from drainage return flows (Simpson and Herczeg 1991).

Carbon isotope

The carbon-14 isotope is used in the study of old hydrological systems. However, the interpretation of radiocarbon data to obtain groundwater absolute ages is largely complicated by the potential mixing with younger and older sources of carbon. (Clark and Fritz 1997; Edmunds and Smedley 2000).

The spatial distribution of the carbon-14 activities, which show a decrease in the direction of flow, demonstrates that the recharge areas are characterized by high carbon-14 activities (111 pm), while the lowest activities characterize the discharge areas (17 pm). The groundwater with high contribution of active organic carbon is characterized by high activities of ^{14}C probably in relation with the infiltration of return flow waters.

The plot of $\delta^{13}C$ versus ^{14}C activity (Fig. 18) suggests that the Grombalia deep groundwater evolves between the pole with high contribution of modern organic carbon, characterized by high activities of ^{14}C (up to 100 pmc) and comparatively low $\delta^{13}C$ values (close to −14 ‰), and the pole characterized by low ^{14}C activities (19.1 pmc) and high values of ^{13}C (−8.87 ‰), reflecting a significant contribution of dead carbon of mineral origin.

The diagram of ^{13}C versus DIC (Fig. 19) shows a positive correlation between these two parameters, apart from a few outliers, indicating that the increase in $\delta^{13}C$ values is accompanied by a general increase in DIC, through water–rock interaction driven conversion of "dead" CO_2 into HCO_3^- ion (Table 2).

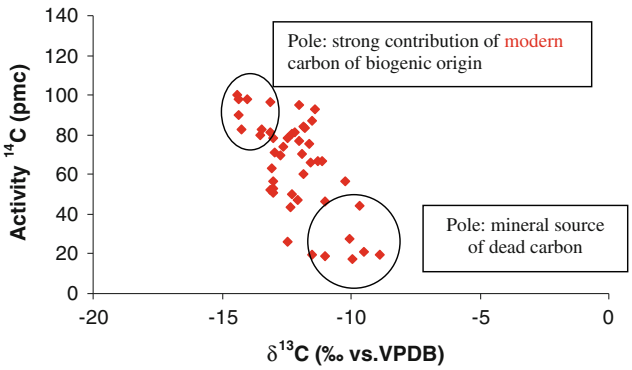

Fig. 18 Correlation diagram of $\delta^{13}C$ values versus DIC ^{14}C activities

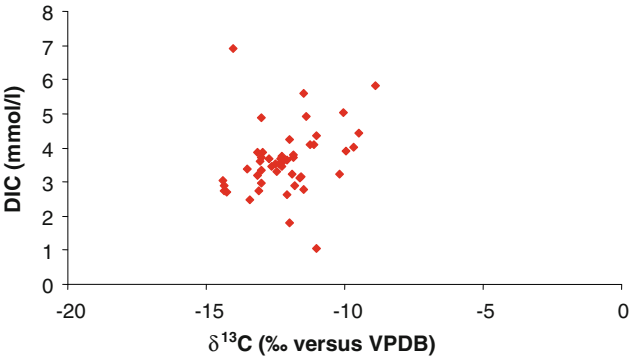

Fig. 19 Correlation diagram of $\delta^{13}C$ values versus DIC concentrations

Table 2 SI data and DIC for Grombalia deep aquifer

No.	SI anhydrite	SI aragonite	SI calcite	SI dolomite	SI gypsum	SI halite	DIC mmol
1	−1.45	0.17	0.32	0.39	−1.23	−5.48	3.72
2	−1.54	0.1	0.25	0.03	−1.31	−5.71	3.86
3	−2.97	−0.24	−0.09	−0.7	−2.73	−6.61	2.74
4	−1.03	−0.02	0.13	−0.25	−0.79	−5.37	3.03
5	−1.45	0.17	0.32	0.07	−1.22	−5.8	2.71
6	−1.85	−0.14	0.01	−0.54	−1.61	−6.27	3.14
7	−1.86	0.37	0.51	1.24	−1.64	−5.81	3.45
8	−1.93	0.33	0.48	0.7	−1.71	−5.99	2.97
9	−1.5	0.16	0.31	0.44	−1.26	−5.52	3.54
10	−2.02	0.18	0.33	0.8	−1.79	−5.83	2.88
11	−1.45	0.07	0.22	0.62	−1.22	−5.45	6.91
12	−2.41	0.02	0.17	0.01	−2.18	−6.22	3.46
13	−1.99	−0.03	0.11	−0.38	−1.76	−6.09	1.82
14	−1.47	−0.73	−0.58	−1.96	−1.23	−5.75	4.11
15	−2.72	−0.13	0.01	−0.12	−2.49	−6.63	3.61
16	−1.84	0.72	0.87	1.63	−1.59	−5.96	3.68
17	−1	0.16	0.3	0.59	−0.77	−6.06	3.24
18	−2.22	0.17	0.31	0.84	−1.99	−7.12	4.91
19	−2.05	0.19	0.34	0.58	−1.83	−6.28	3.62
20	−2.29	0.2	0.34	0.51	−2.06	−7.45	3.66
21	−1.58	0.43	0.58	1.06	−1.36	−6.15	3.19
22	−1.77	0.74	0.88	1.32	−1.54	−6.29	5.60
23	−2.16	0.15	0.3	0.58	−1.93	−6.26	3.40
24	−1.39	0.31	0.45	0.55	−1.16	−5.46	3.31
25	−1.58	−0.06	0.08	0.24	−1.35	−5.53	4.08
26	−1.75	−0.05	0.1	0.56	−1.54	−5.98	3.36
27	−0.89	0.38	0.53	1.28	−0.66	−5.01	3.63
28	−2.45	0.18	0.33	0.8	−2.21	−6.31	3.74
29	−1.34	0.1	0.25	0.58	−1.11	−5.6	2.73
30	−1.47	0.08	0.23	0.47	−1.23	−5.7	2.48
31	−1.4	0.19	0.34	0.47	−1.17	−5.54	3.80
32	−1.14	0.06	0.21	0.16	−0.91	−5.57	2.65
33	−2.15	0.19	0.34	0.09	−1.92	−6.69	4.35
34	−1.84	−0.03	0.11	0.04	−1.6	−6.08	3.55
35	−1.19	0.27	0.42	0.4	−0.96	−5.63	3.15
36	−1.02	0.49	0.63	1.17	−0.78	−4.85	2.78
37	−0.64	0.45	0.59	0.8	−0.41	−4.56	3.91
38	−1.14	0.66	0.81	0.99	−0.91	−5.55	3.22
39	−2.05	0.66	0.81	1.43	−1.82	−7	3.70
40	−1.08	0.38	0.53	0.96	−0.84	−5.51	4.00
41	−2.08	−0.18	−0.04	−0.05	−1.85	−6.64	3.87
42	−2.1	0.55	0.7	1.37	−1.86	−6.78	4.44
43	−2.34	−0.19	−0.05	0.08	−2.11	−6.81	5.83
44	−1.8	0.72	0.86	1.89	−1.56	−5.83	5.02
45	−1.03	−0.18	−0.03	−0.06	−0.8	−5.42	4.90
46	−1.06	0.1	0.25	0.39	−0.83	−5.13	2.88
47	−1.94	0.04	0.19	0.37	−1.7	−6.07	4.24
48	−1.42	0.31	0.46	1.08	−1.2	−5.21	1.06

Table 2 continued

No.	SI anhydrite	SI aragonite	SI calcite	SI dolomite	SI gypsum	SI halite	DIC mmol
49	−1.5	0.16	0.31	0.51	−1.27	−5.13	3.72
50	−1.22	0.1	0.25	0.27	−1	−5.48	3.86
51	−1.6	0.43	0.58	1.06	−1.36	−5.45	2.74
52	−1.05	0.27	0.41	0.7	−0.81	−5.4	3.03
53	−1.52	0.49	0.64	1.01	−1.29	−5.47	2.71
54	−1.77	0.2	0.36	0.41	−1.52	−5.82	3.14
55	−2.02	0.02	0.16	0.46	−1.79	−6.45	3.45

Conclusion

The study area of Grombalia, located in the northeast of Tunisia, is most important in the Cap Bon area since it is used to meet the increasing water demand for agricultural, industrial and tourist activities.

Combined use of hydrochemistry and isotopic composition of groundwater samples collected from the Grombalia multilayer aquifer allowed a detailed insight into the active processes.

The chemical composition of groundwater is chiefly controlled by incongruent dissolution of gypsum and halite, rock dissolution reactions driven by conversion of aqueous CO_2 into HCO_3^- ion, precipitation of calcite and cation exchange.

Additionally, the return flow process in relation to the long-term flood irrigation practice contributes to mineralization by producing high amounts of nitrate.

The correlation diagrams of $\delta^{18}O$ versus $\delta^{2}H$ reveals the existence of two groundwater groups: (1) the non-evaporated groundwater, representative of meteoric recharge, and (2) the evaporated groundwater, reflecting the influence of return flow of irrigation water.

Based on the Gonfiantini (1986) equation, the fraction of evaporated water from the Grombalia aquifer ranges between 0.24 and 0.65%, based on ^{18}O. These expected results reflect the semi-arid conditions prevailing in the study area.

Acknowledgments The authors wish to thank the Laboratory of the International Agency of Atomic Energy (IAEA) for the financial support provided to the Technical Cooperation Project (TUN 8/019) within which this work was carried out. We thank the staff members of Nabeul Water Resources Division/Agriculture Ministry.

References

Abid K, Zouari K, Dulinski M, Chkir N (2009) Hydrologic and geologic factors controlling groundwater geochemistry in the Turonian aquifer (southern Tunisia) Journal of Environ Earth Sci 19:415–427

Appelo CAJ, Postma D (1993) Geochimistry. Groundwater and Pollution, Balkema, Rotterdam

Ben Ayed N (1986) Evoulution tectonique de l'avant-pays de la chaine alpine de la Tunisie du début de Mésosoique à l'actuel. Thèse de Doctorat es-Science, Univ, Paris Sud. Orsay 347

Ben Hamouda MF, Tarhouni J, Leduc C, Zouari K (2010) Understanding the origin of salinization of the Plio-Quaternary eastern coastal aquifer of Cap Bon (Tunisia) using geochemical and isotope investigations. Environ Earth Sci J 63:889–901

Ben Salem H (1992) Contribution à la connaissance de la géologie du Cap Bon: stratigraphie, tectonique et sédimentologie. Thèse 3éme cycle, Géol. Univ. Tunis II

Bouchaou L, Michelot JL, Vengosh A, Hsissou Y, Qurtobi M, Gaye CB, Bullen TD, Zuppi GM (2008) Application of multiple isotopic and geochemical tracers for investigation of recharge, salinization, and residence time of water in the Souss-Massa aquifer, southwest of Morocco. J Hydrol 352:267–287

Carol E, Kruse E, Mas-pla J (2009) Hydrochemical and isotopical evidence of groundwater salinization process on the coastal plain of Samborombon Bay, Argentina. J Hydrol 365:335–345

Castany G (1948) Les fossés d'effondrement de Tunisie. Géologie et hydrogéologie. 1°fasc. Plaine de Grombalia et cuvettes de Tunisie orientale. Ann. Mines et Géol. Tunis, N° 3, pp 18–39

Clark I, Fritz P (1997) Environmental Isotopes in Hydrogeology. Lewis Publishers, Boca Raton, Florida

Coleman ML, Shepherd TJ, Durham JJ, Rouse JE, Moore GR (1982) Reduction of water with zinc for hydrogen isotope analysis. Anal Chem 54:993–995

Coplen TB (1996) New guidelines for reporting stable hydrogen, carbon, and oxygen isotope-ratio data. Geochim Cosmochim Acta 60:3359–3360

Craig H (1961) Standards for reporting concentrations of deuterium and oxygen-18 in natural waters. Science 133:1833–1834

DGRE (2000) Annuaires de l'exploitation des ressources en eau. Direction générale des ressources en eaux, Tunis

Edmunds WM, Smedley PL (2000) Residence time indicators in groundwater: the East Midlands Triassic sandstone aquifer. Appl Geochem 15:737–752

Edmunds WM, Bath AH, Miles DL (1982) Hydrochemical evolution of the East Midlands Triassic sandstone aquifer, England. Geochim Acta 46:2069–2081

Ennabli M (1980) Etat hydrogéologique des aquifères du Nord-Est de la Tunisie pour une gestion intégrée des ressources en eaux. Thèse Doct. Es-Sci. Nice

Epstein S, Meyada TK (1953) Variations of ^{18}O content of waters from natural sources. Geochim Cosmochim Acta 4:213–224

Etcheverry D (2002) Valorisation des méthodes isotopiques pour les questions pratiques liées aux eaux souterraines. Office fédéral des eaux et de la géologie, Lausanne

Fontes JC (1971) Un ensemble destiné à la mesure de l'activité du radiocarbone naturel par scintillation liquide. Rev Geog Phys Géol Dyn 13(1):67–86

Fontes JC (1980) Environmental isotopes in groundwater hydrology. In: Fritz P, Fontes JC (eds) Handbook of environmental isotope geochemistry. Elsevier, Amsterdam, pp 75–140

Geyh MA (2000) An overview of 14C analysis in the study of groundwater. Radiocarbon 42(1):99–114

Gonfiantini R (1986) Environmental isotopes in lake studies. In: Fritz P, Fontes JC (eds) Handbook of Environmental Isotope Geochemistry, The Terrestrial Environment B, Vol II. Elsevier, Amsterdam, pp 113–168

Hao X, Change C (2002) Does long-term heavy cattle manure application increase salinity of a clay loam soil in semi-arid southern Alberta? Agric Ecosys Environ 1934:1–16

Hern J, Feltz HR (1998) Effects of irrigation on the environment of selected areas of the Western United States and implications to world population growth and food production. J Environ Manag 52:353–360

Kattan Z (2007) Estimation of evaporation and irrigation return flow in arid zones using stable isotope ratios and chloride mass-balance analysis: case of the Euphrates River, Syria. J Arid Environ 72:730–747

Mahmoudi S (2005) Etude hydrogéologique, hydrochimique et isotopique de la nappe profonde de Grombalia (Tunisie). Master de Sciences de la Terre et de l'univers (DEA), spécialité Hydrologie–Hydrogéologie-sols à l'Université Paris-Sud 11; Faculté des Sciences d'Orsay, France

Plummer LN, Jones BF, Truesdell AH (1976) WATEQ, a Fortan IV version of WATEQ, a computer program for calculating chemical equilibrium of natural waters. US Geol Surv Water Resour Invest 76:61

Simpson HJ, Herczeg AL (1991) Salinity and evaporation in the river Murray Basin, Australia. J Hydrol 124:1–27

Stigter TY, Carvalho AM, Ribeiro L, Reis E (2006) Impact of the shift from groundwater to surface water irrigation on aquifer dynamics and hydrochemistry in a semi-arid region in the south of Portugal. Agric Water Manag 85:121–132

Touati MA, Brehem JA, Tenhave LE (1994) Tectonic development of the Belli field area. Proceeding of the 4th Tunisian petroleum exploration conference. Tunis, May 1994, pp 365–378

Yangui H, Zouari K, Trabelsi R, Rozanski K (2010) Recharge mode and mineralization of groundwater in a semi-arid region: Sidi Bouzid Plain (central Tunisia) Journal of Environ Earth Sci 63:969–979

Zouari K, Aranyossy JF, Mamou A, Fontes JCh (1985) Etude isotopique et géochimique des mouvements et de l'évolution dessolutions de la zone aérée des sols sous climat semi-aride (Sud tunisien). In: Stable and Radioactive Isotopes in the Study of the Unsaturated Soil Zone. Proceedings of the final meeting of the joint IAEA/GSF co-ordinated research programme for studying the physical and isotopic behaviour of soil moisture in the zone of aeration, organized by the International Atomic Energy Agency and Held, Vienna, pp 121–144